Protonation of the oxide bridge is known to reduce the magnitude of the antiferromagnetic interaction. For example, protonation of the oxide bridge in $[(HB(pz)_3Fe)_2O(OAc)_2]$ to give $[(HB(pz)_3Fe)_2(OH)(OAc)_2]^+$ changes J from -121 to $J = -17$ cm^{-1}. The Fe–O bond distance also increases from 1.784 to 1.956 Å.[1a] In fact, hydrogen-bonding contacts involving an oxide bridge between two Fe^{III} ions have been suggested for proteins with binuclear iron sites.[1a,c,25] In the case of oxyhemerythrin (oxy-Hr) a hydroperoxide ($O-O-H^-$) ligand coordinated to one Fe^{III} ion is believed to be involved in a hydrogen-bonding contact interaction with the oxide bridge. For oxyHr a J value of -77 cm^{-1} is found, which is to be compared to -134 cm^{-1} for Fe_2^{III} metHr. A hydrogen-bonding contact interaction has also been suggested for the $\overset{\lceil O \rceil}{Fe^{III}Fe^{III}}$ bridge in the ribonucleotide reductase from *E. coli*.

Acknowledgment. This work was supported by the NIH Grant HL13652 to D.N.H. and the NSF Grant CHE8808019 to G.C.

Supplementary Material Available: Complete listings of bond distances and angles, anisotropic thermal parameters, and magnetic susceptibility data for $[Fe_4O_2(O_2CCH_3)_7(bpy)_2](ClO_4)\cdot {}^1/_4CH_2Cl_2\cdot H_2O$ (**1**) (6 pages); tables of observed and calculated structure factors (8 pages). Ordering information is given on any current masthead page. A complete structure report for complex **1** (No. 88019) is available upon request from the Indiana University Chemistry Library.

Heteronuclear ^{13}C–^1H NMR Investigation of the Effects on an Oligodeoxyribonucleotide of Intrastrand Cross-Linking by a Pt Anticancer Drug. A Large Shift of C3′ Accompanies an S to N Conformational Change

Srinivasan Mukundan, Jr.,[†] Yinghai Xu,[†] Gerald Zon,[‡] and Luigi G. Marzilli*,[†]

Contribution from the Department of Chemistry, Emory University, Atlanta, Georgia 30322, and Applied Biosystems, Foster City, California 94404. *Received September 4, 1990*

Abstract: NMR spectral characterization of DNA and RNA oligonucleotides with unusual structural features may be impeded by the absence of NOE connectivities in the 2D homonuclear proton NOESY spectrum. Furthermore, in larger oligonucleotides, signal overlap may prevent an accurate measurement of the homonuclear coupling constants necessary to assess average sugar conformation. As part of an ongoing study of the effects of platinum anticancer drugs on deoxyribonucleotides, we examined the use of ^{13}C NMR spectroscopy on the model systems, $d(T_1G_2G_3T_4)$ and $[d(T_1G_2G_3T_4)N7,N7]$-Pt(en), where en = ethylenediamine and the N7 of both G's is attached to the metal. Such an intrastrand cross-link adduct is the major lesion formed when such anticancer drugs bind to DNA. These oligonucleotides were examined with both heteronuclear multiple-quantum coherence (HMQC) and heteronuclear multiple-bond correlation (HMBC) spectroscopy. Intranucleotide heteronuclear scalar connectivities were observed between the H1′ and the pyrimidine base C2 and C6 signals and the pyrimidine H6 and deoxyribose C1′ signals, thereby circumventing the need to rely on the less certain NOE connectivities to identify the base and sugar signals of the same nucleotide. For the parent oligonucleotide, a similar set of heteronuclear couplings was observed for the H1′, C8, and C4 signals of the purine nucleotides. However, for $[d(T_1G_2G_3T_4)$-$N7,N7]$-Pt(en), these latter connectivities were not observed, a result consistent with a structural distortion caused by platination. Nevertheless, the purine base ^{13}C signals gave the characteristic pattern of shift changes expected for N7 metalation predicted on the basis of past studies on mononucleotides. The method should be useful in identifying metalation sites in oligonucleotides. Comparison of solid-state ^{13}C data for deoxyribose moieties in the N and the S conformations leads to the prediction that the ^{13}C signals will undergo appreciable shift changes in any transformation that induces an S to N conformational change. We found that, at 12 °C, the C3′ signal of G_2 in $d(T_1G_2G_3T_4)$ was shifted upfield by 6.6 ppm in $[d(T_1G_2G_3T_4)$-$N7,N7]$-Pt(en), consistent with such a conformational change. Of considerable interest, the H1′ signal of G_2 $[d(T_1G_2G_3T_4)$-$N7,N7]$-Pt(en) was broad at 12 °C; it shifted downfield and sharpened with an increase in temperature to 40 °C. No appreciable changes were observed in the ^{13}C shifts, suggesting that the characteristic behavior of the H1′ signal of the 5′G in such cross-links is not the result of a significant change in the average conformation of the deoxyribose moiety but may be due to changes in the orientation of the bases with respect to the deoxyribose and/or the Pt coordination sphere.

Introduction

Modern 2D NMR spectroscopy is gaining ever-increasing application to the study of biomolecules.[1] NMR studies of oligonucleotides can provide insight into unusual structures present in DNA or RNA, such as hairpins and bulges, or novel structures formed by the treatment of DNA with anticancer drugs or intercalators.[2-9] Most studies have utilized ^1H NMR spectroscopy, while fewer studies have examined other nuclei, particularly ^{31}P.[9] Although ^1H NMR spectra of regular duplex DNA structures can be assigned with little difficulty, conformationally flexible structures, such as single-stranded DNA or those induced by anticancer compounds, may not have all the necessary ^1H–^1H NOE cross peaks for sequential assignments.[5] Increased emphasis is now being placed on ^{13}C NMR spectroscopy of oligonucleotides

[†] Emory University.
[‡] Applied Biosystems.

(1) Wüthrich, K. *NMR of Proteins and Nucleic Acids*; John Wiley & Sons: New York, 1986. See also: Live, D., Armitage, I. M., Patel, D., Eds. *Frontiers of NMR in Molecular Biology*; Wiley-Liss: New York, 1990.
(2) Wemmer, D. E.; Chou, S. H.; Hare, D. R.; Reid, B. R. *Nucleic Acids Res.* **1985**, *13*, 3755. Hare, D. R.; Reid, B. R. *Biochemistry* **1986**, *25*, 5341. Ikuta, S.; Chattopadhyaya, R.; Ito, H.; Dickerson, R. E.; Kearns, D. R. *Biochemistry* **1986**, *25*, 4840. Orbons, L. P. M.; van Beuzekom, A. A.; Altona, C. *J. Biomol. Struct. Dyn.* **1987**, *4*, 965. Summers, M. F.; Byrd, R. A.; Gallo, K. A.; Samson, C. J.; Zon, G.; Egan, W. *Nucleic Acids Res.* **1985**, *13*, 6375.
(3) Roy, S.; Sklenar, V.; Appella, E.; Cohen, J. S. *Biopolymers* **1987**, *26*, 2041. Nikonowicz, E. P.; Meadows, R. P.; Gorenstein, D. G. *Biochemistry* **1990**, *29*, 4193. Hare, D.; Shapiro, L.; Patel, D. J. *Biochemistry* **1986**, *25*, 7456. van den Hoogen, Y. Th.; van Beuzekom, A. A.; de Vroom, E.; van der Marel, A.; van Boom, J. H.; Altona, C. *Nucleic Acids Res.* **1988**, *16*, 5013.

0002-7863/91/1513-3021$02.50/0

because of the greater dispersion of ^{13}C shifts compared to either ^{1}H or ^{31}P shifts. Nevertheless, relatively few studies have been reported in this new area of the application of ^{13}C NMR spectroscopy,[10] primarily due to the insensitivity of the ^{13}C nucleus.

We are particularly interested in adducts formed between DNA and the very important *cis*-PtA_2X_2 class of anticancer compounds, with two cis amine ligands (A) or a bidentate diamine chelate (A_2) and two cis leaving ligands (X) or a leaving bidentate ligand (X_2).[11-13] The adducts formed between *cis*-$Pt(NH_3)_2Cl_2$, a widely used drug, and N7 of guanine are the principal series formed on reaction of the drug with DNA, the likely molecular target responsible for anticancer activity. The major adduct, an N7,N7 intrastrand cross-link between two adjacent guanines,[12] can cause pronounced structural changes in DNA.[5,13]

Recent papers suggest that ^{13}C NMR spectroscopy can be particularly useful in studying Pt(II) interactions with oligonucleotides. For example, the $^{13}C-^{1}H$ coupling constant for C8–H8 guanine nucleosides in DMSO-d_6 has been reported to increase from ~215 to ~220 Hz on N7 platination.[14] There are also upfield and downfield shifts of the C5 and C8 signals, respectively. Such Pt adducts also can change the sugar pucker, but unusual changes in ^{1}H shifts and poorly resolved ^{1}H coupling patterns are often observed.[5-8] In a recent important and extensive study, Harbison and co-workers used solid-state ^{13}C NMR spectroscopy to correlate ^{13}C NMR shifts with sugar pucker.[15] Although interpretation of ^{13}C NMR shifts requires considerable caution, dramatic differences were observed for the same type sugar carbon in residues with different pucker. In particular, the C3′ signal is predicted to shift ~8 ppm upfield for a C2′ endo → C3′ endo conversion. Harbison and co-workers suggested that ^{13}C NMR shifts could find utility in solution-state studies.

We have explored the application of some of these observations to aqueous solutions with the model system [5′d(TGGT)3′-*N7,N7*]-Pt(en). Hereafter, this adduct will be referred to as d(TGGT)-Pt(en), where en = ethylenediamine. Other *cis*-PtA_2 analogues give similar adducts, and this derivative was chosen to explore the utility of ^{13}C NMR spectroscopy because the ^{1}H and ^{31}P spectra of this adduct were previously investigated in depth with both 1D and 2D methods.[8] The Pt(en) derivative also exhibits the characteristically broad H1′ signal of the 5′-platinated G.[5-8] Of the relatively few ^{13}C NMR studies of oligonucleotides that have been reported, we are unaware of any involving anticancer drug adducts.

Experimental Section

2D NMR of d(TGGT). The oligodeoxyribonucleotide 5′d(TGGT)3′ was prepared and purified as previously described.[8] For 2D NMR spectroscopy, a 500-μL sample 63 mM in bases was dissolved in D_2O and the pD corrected to 6.0 (pH 5.6). The sample was then lyophilized from 99.9% D_2O three additional times before final dissolution in an equal amount of high-grade (99.96%) D_2O obtained from ICN. Two-dimensional NMR experiments were performed on a General Electric GN 500 NMR spectrometer operating at 500.1 MHz for ^{1}H (125.76 MHz, ^{13}C). All 2D experiments were performed at 12 °C without sample spinning. High-resolution 1D ^{13}C spectroscopy was performed at ambient temperature (22 °C) on a General Electric QE 300 NMR spectrometer operating at 74.8 MHz. The internal standard sodium 3-(trimethylsilyl)propionate-*2,2,3,3-d*$_4$ (TSP) was employed as a chemical shift reference for both ^{1}H and ^{13}C spectroscopy.

(a) COSY. The absolute value correlation spectroscopy (COSY) spectrum[16] resulted from a 512 × 2048 matrix, summing 32 scans per t_1 increment. Resolution was enhanced by broad-band decoupling the ^{31}P frequency range, thereby eliminating ^{31}P couplings to the H3′, H5′, and H5″ protons and reducing the complexity of the spectrum. A 0.5-s relaxation delay and a 2.5-s solvent presaturation pulse were used prior to each acquisition. The data were processed on a DEC Microvax II computer with the FTNMR software (Hare Research, Inc., Woodinville, WA). Gaussian multiplication with line broadening of −1.0 Hz and Gaussian broadening of 0.1 Hz followed by a sine-bell filter was applied in the t_2 dimension prior to Fourier transformation. A sine-bell-squared apodization function was applied in the t_1 dimension. The data were zero filled to 1024 data points prior to Fourier transformation.

(b) NOESY. The phase-sensitive nuclear Overhauser enhancement spectroscopy (NOESY) spectrum[17] resulted from a 2 × 512 × 2048 data point matrix size with 16 scans per t_1 increment. Each acquisition was preceded by a 0.5-s relaxation delay and a 2.5-s presaturation pulse, which eliminated residual solvent HOD signal. The data were processed by exponential multiplication with line broadening of 3 Hz in the t_2 dimension. The t_1 dimension was zero filled to 1024 data points and a 90° shifted squared sine-bell filter applied to the first 512 data points prior to Fourier transformation.

(c) HMQC. The single-bond $^{1}H-^{13}C$ heteronuclear multiple-quantum coherence (HMQC) spectrum[18] resulted from a matrix of 256 × 2048 data points with 256 acquisitions per t_1 increment. A 1.0-s relaxation delay was used between scans. A 38-μs 90° ^{13}C pulse width requiring 43 W of rf power was utilized in the experiment. The data were processed by Gaussian multiplication with line broadening of −1.0 and 0.1 Hz of Gaussian broadening followed by a sine-bell filter prior to Fourier transformation in the t_2 dimension. The t_1 dimension was apodized with a 90° shifted squared sine bell applied to the first 256 data points. The data were then zero filled to 1024 data points and Fourier transformed. Coupling constants were computed from one-dimensional slices from the 2D data set.

(d) HMBC. The $^{1}H-^{13}C$ heteronuclear multiple-bond correlation (HMBC) spectrum[19] resulted from a matrix of 512 × 1024 data points

(4) Scott, E. V.; Zon, G.; Marzilli, L. G.; Wilson, W. D. *Biochemistry* **1988**, *27*, 7940; Gao, X.; Patel, D. J. *Biochemistry* **1988**, *27*, 1744. Marzilli, L. G.; Banville, D. L.; Zon, G.; Wilson, W. D. *J. Am. Chem. Soc.* **1986**, *108*, 4188. Wilson, W. D.; Jones, R. L.; Zon, G.; Banville, D. L.; Marzilli, L. G. *Biopolymers* **1986**, *25*, 1997. Strickland, J. A.; Marzilli, L. G.; Wilson, W. D.; Zon, G. *Inorg. Chem.* **1989**, *28*, 4191.

(5) Kline, T. P.; Marzilli, L. G.; Live, D.; Zon, G. *J. Am. Chem. Soc.* **1989**, *111*, 7057, and references cited therein. den Hartog, J. H. J.; Altona, C.; van Boom, J. H.; van der Marel, G. A.; Haasnoot, C. A. G.; Reedijk, J. *J. Biomol. Struct. Dyn.* **1985**, *2*, 1137. Kline, T. P.; Marzilli, L. G.; Live, D.; Zon, G. *Biochem. Pharmacol.* **1990**, *40*, 97.

(6) Caradonna, J. P.; Lippard, S. J. *Inorg. Chem.* **1988**, *27*, 1454, and references cited therein.

(7) Neumann, J.-M.; Tran-Dinh, S.; Girault, J.-P.; Chottard, J.-C.; Huynh-Dinh, T.; Igolen, J. *Eur. J. Biochem.* **1984**, *141*, 465. den Hartog, J. H. J.; Altona, C.; van der Marel, G. A.; Reedijk, J. *Eur. J. Biochem.* **1985**, *147*, 371. Xu, Y.; Natile, G.; Intini, F. P.; Marzilli, L. G. *J. Am. Chem. Soc.* **1990**, *112*, 8177. See also: Reference 22.

(8) Fouts, C. S.; Marzilli, L. G.; Byrd, R. A.; Summers, M. F.; Zon, G.; Shinozuka, K. *Inorg. Chem.* **1988**, *27*, 366. Byrd, R. A.; Summers, M. F.; Zon, G.; Fouts, C. S.; Marzilli, L. G. *J. Am. Chem. Soc.* **1986**, *108*, 504.

(9) Williamson, J. R.; Boxer, S. G. *Biochemistry* **1989**, *28*, 2819. Williamson, J. R.; Boxer, S. G. *Biochemistry* **1989**, *28*, 2831. Fouts, C. S.; Reily, M. D.; Marzilli, L. G.; Zon, G. *Inorg. Chim. Acta* **1987**, *137*, 1. den Hartog, J. H. J.; Altona, C.; van Boom, J. H.; Reedijk, J. *FEBS Lett.* **1984**, *176*, 393. Nikonowicz, E.; Roongta, V.; Jones, C. R.; Gorenstein, D. G. *Biochemistry* **1989**, *28*, 8714. Gorenstein, D. G.; Goldfield, E. M. *Phosphorus-31 NMR: Principles and Applications*; Academic Press: New York, 1984.

(10) LaPlante, S. R.; Boudreau, E. A.; Zanatta, N.; Levy, G. C.; Borer, P. N.; Ashcroft, J.; Cowburn, D. *Biochemistry* **1988**, *27*, 7902. Ashcroft, J.; LaPlante, S. R.; Borer, P. N.; Cowburn, D. *J. Am. Chem. Soc.* **1989**, *111*, 363. Borer, P. N.; LaPlante, S. R.; Zanatta, N.; Levy, G. C. *Nucleic Acids Res.* **1988**, *16*, 2323. Borer, P. N.; Ashcroft, J.; Cowburn, D.; Levy, G. C.; Borer, P. N. *J. Biomol. Struct. Dyn.* **1988**, *5*, 1089. Zanatta, N.; Borer, P. N.; Levy, G. C. *Recent Advances in Organic NMR Spectroscopy*; Lambert, J. B., Rittner, R., Eds.; Norell: Landisville, NJ, 1987; p 89. Live, D. In *Frontiers of NMR in Molecular Biology*; Live, D., Armitage, I. M., Patel, D., Eds.; Wiley-Liss: New York, 1990; p 259.

(11) Leh, F. K. V.; Wolf, W. *J. Pharm. Sci.* **1976**, *65*, 315. Johnson, N. P.; Butour, J.-L.; Villani, G.; Wimmer, F. L.; Defais, M.; Pierson, V.; Brabec, V. *Prog. Clin. Biochem. Med.* **1989**, *10*, 1. Inagaki, K.; Kidani, Y. *Inorg. Chem.* **1986**, *25*, 1. Roberts, J. J. *Adv. Inorg. Biochem.* **1981**, *3*, 273.

(12) Fichtinger-Schepman, A. M. J.; van der Veer, J. L.; den Hartog, J. H. J.; Lohman, P. H. M.; Reedijk, J. *Biochemistry* **1985**, *24*, 707. Inagaki, K.; Kasuya, K.; Kidani, Y. *Chem. Lett.* **1984**, 171. Fichtinger-Schepman, A. M. J.; van Oosterom, A. T.; Lohman, P. H. M.; Berends, F. *Cancer Res.* **1987**, *47*, 3000.

(13) Rice, J. A.; Crothers, D. M.; Pinto, A. L.; Lippard, S. J. *Proc. Natl. Acad. Sci. U.S.A.* **1988**, *85*, 4158. Reedijk, J.; Fichtinger-Schepman, A. M. J.; van Oosteroom, A. T.; van de Putte, P. *Struct. Bonding* **1987**, *67*, 53. Sherman, S. E.; Lippard, S. J. *Chem. Rev.* **1987**, *87*, 1153.

(14) Barbarella, G.; Bertoluzza, A.; Morelli, M. A.; Tosi, M. R.; Tugnoli, V. *Gazz. Chim. Ital.* **1988**, *118*, 637.

(15) Santos, R. A.; Tang, P.; Harbison, G. S. *Biochemistry* **1989**, *28*, 9372.

(16) Aue, W. P.; Bartholdi, E.; Ernst, R. R. *J. Chem. Phys.* **1976**, *64*, 2229. Bax, A.; Freeman, R. *J. Magn. Reson.* **1981**, *4*, 542.

(17) Jeener, J.; Meier, B. H.; Bachmann, P.; Ernst, R. R. *J. Chem. Phys.* **1979**, *71*, 4546. Kumar, A.; Ernst, R. R.; Wüthrich, K.; *Biochem. Biophys. Res. Commun.* **1980**, *95*, 1. States, D. J.; Haberkorn, R. A.; Ruben, D. J. *J. Magn. Reson.* **1982**, *48*, 286.

(18) Müller, L. *J. Am. Chem. Soc.* **1979**, *101*, 4481. Bax, A.; Subramanian, S. *J. Magn. Reson.* **1986**, *67*, 565. Live, D. H.; Davis, D. G.; Agosta, W. C.; Cowburn, D. *J. Am. Chem. Soc.* **1984**, *106*, 1939.

(19) Bax, A.; Summers, M. F. *J. Am. Chem. Soc.* **1986**, *108*, 2093.

with 128 acquisitions per t_1 increment, and a 1.0-s relaxation delay. A 90° ^{13}C pulse width resulting from 43 W of rf power for 38 μs was utilized. The values of Δ_1 (the delay between the first 90° ^1H pulse and the first 90° ^{13}C pulse) was 3.3 ms, and the value of Δ_2 (the delay between the first and second 90° ^{13}C pulses) was 50 ms. The data were processed by Gaussian multiplication with line broadening of −2.0 and 0.2 Hz of Gaussian broadening prior to Fourier transformation in both dimensions.

2D NMR of d(TGGT)-Pt(en). Platinated samples for 2D NMR analysis were typically prepared by using the following conditions in D_2O: 10 mM in bases, 2.5 mM Pt(en)Cl_2, pD 6.0, T = 12.0° C. The reaction was followed by NMR, with quantitative product formation in approximately 1 week. The dilute reaction mixture was concentrated, yielding a 500-μL sample 60 mM in bases. The pD of the sample was corrected to 6.0, and the sample lyophilized three additional times from 99.9% D_2O. A full complement of 2D NMR spectra was acquired at 12 °C as described above, with additional homonuclear Hartmann–Hahn, HMQC, and HMBC spectra acquired at 40 °C. Differences between the above NMR acquisitions and those for the platinated species are described below.

(a) COSY. The absolute value COSY spectrum resulted from a 400 × 1024 matrix with 32 accumulations per t_1 increment. A 3.0-s solvent presaturation pulse was used prior to each scan. A Gaussian filter (Gaussian broadening 0.4 Hz, line broadening −2 Hz) was applied to the t_2 data. The t_1 data were processed by using a sine-bell function on the first 400 data points.

(b) NOESY. The phase-sensitive NOE spectrum resulted from a 2 × 400 × 2048 matrix, summing 32 scans per t_1 period. Each acquisition was preceded by a 3-s solvent presaturation pulse. An exponential multiplication window was applied to the t_2 data. The t_1 data were zero filled to 1024 data points, followed by application of a 90° shifted sine-bell-squared function.

(c) HOHAHA. The phase-sensitive homonuclear Hartmann–Hahn spectrum[20] resulted from a 2 × 400 × 2048 matrix, with 64 scans per t_1 increment. A 1.0-s relaxation delay, and a MLEV-17 spin–lock sequence of 179.38 ms was used. A 60.4-μs 90° pulse width required 6 W of power. The t_2 data were processed by using a Gaussian filter with Gaussian broadening of 0.2 Hz and line broadening of −1.0 Hz. The t_1 data were zero filled to 512 data points. The first 400 data points were multiplied with a 90° shifted sine-bell window.

(d) HMQC. The HMQC spectrum resulted from a matrix of 128 × 1024 data points, summing 448 scans per t_1 increment. A 38-μs 90° ^{13}C pulse width requiring 43 W of rf power was utilized in the experiment, and a 1.0-s relaxation delay was used between scans. The t_2 data were apodized with a Gaussian filter (Gaussian broadening 0.2 Hz, line broadening −1.0 Hz), followed by a 90° shifted sine-bell filter prior to Fourier transformation. The t_1 data were zero filled to 512 data points, with a 90° shifted sine-bell filter applied to the first 128 data points.

(e) HMBC. The HMBC spectrum resulted from a 256 × 1024 matrix, adding 440 acquisitions per block. A 90° ^{13}C pulse width resulting from 43 W of rf power for 38 μs and a 1-s relaxation delay were utilized. A Gaussian filter (Gaussian broadening 0.2 Hz, line broadening −1.0 Hz) was used to apodize the t_2 data. The t_1 data were zero filled to 512 data points, with a 90° shifted sine-bell filter applied to the first 256 data points.

Results

Assignment of ^1H NMR Signals of d(TGGT). Assignment of the signals of the nonexchangeable base protons and sugar protons of the single-stranded tetranucleotide d(TGGT) was possible through 2D NOESY and COSY techniques (Table I). The following numbering scheme is used: 5′d($T_1G_2G_3T_4$)3′. Unfortunately, the standard technique of sequentially assigning the base proton resonances to specific bases by making use of 2D NOE base proton to sugar H1′ connectivities[1] could not be used, since only six of seven expected cross peaks were observed. Sequential assignments began with the T H6 protons. A cross peak observed from the characteristically upfield shifted (~0.5 ppm) H5′/H5″ signal of the nonphosphorylated 5′-end sugar to the resonance at 7.40 ppm facilitated assignment of this signal to T_1 H6. The other T H6 resonance, T_4 H6, shows connectivity to its own H1′, which has a connectivity to the signal at 7.98 ppm assigning it to G_3 H8. The remaining sugars were assigned in the usual manner (Table I).

(20) Braunschweiler, L.; Ernst, R. R. *J. Magn. Reson.* **1983**, *53*, 521. Davis, D. G.; Bax, A. *J. Am. Chem. Soc.* **1985**, *107*, 2820. Bax, A.; Davis, D. G. *J. Magn. Reson.* **1985**, *65*, 355.

Table I. ^1H Chemical Shifts (ppm) of d(TGGT) (**1**) and d(TGGT)-Pt(en) (**2**) at 12 °C[a]

	atom type							
	T_1		G_2		G_3		T_4	
	1	**2**	**1**	**2**	**1**	**2**	**1**	**2**
				Sugars				
H1′	6.02	6.03	5.84	5.88	6.08	6.24	6.20	6.27
H2′[b]	1.65	1.89	2.58	2.79	2.69	2.70	2.30	2.35
H2″[b]	2.21	2.24	2.64	2.39	2.78	2.77	2.30	2.35
H3′	4.63	4.48	4.97	5.24	5.02	5.01	4.60	4.59
H4′	4.04	3.94	4.33	4.26	4.42	4.44	4.11	4.14
H5′[c]	3.64	3.68	3.97	4.06	4.19	3.99	4.23	4.19
H5″[c]	3.64	3.68	4.07	4.06	4.19	4.16	4.23	4.21
				Bases				
H6	7.40	7.57					7.52	7.64
H8			7.86	8.12	7.99	9.03		
Me	1.84	1.85					1.75	1.78

[a] The ethylenediamine resonances are observed at 2.92 and 2.83 ppm. [b] H2′ is assigned to the upfield signal of the H2′, H2″ geminal pair. [c] H5′ is assigned to the upfield signal of the H5′, H5″ geminal pair.

Assignment of the ^{13}C NMR Signals of Protonated Carbon Atoms in d(TGGT). The 2D HMQC method gives signals for all protonated carbon atoms through ^1H–^{13}C single-bond couplings. Moreover, the separation (in hertz) between the two correlations observed in the ^1H dimension for each ^{13}C signal gives the ^1H–^{13}C single-bond coupling constant. The 2D HMQC ^{13}C shifts reported in Table II compare favorably with those in the high-resolution 1D spectrum.

The ^{13}C assignment is straightforward, given the complete ^1H assignment. Additionally, the ^{13}C assignment provides independent verification of the ^1H assignments. For example, an upfield shift is characteristic of the 5′-terminal C5′ carbon.[10] The correlation of the upfield shifted C5′ atom at 64.06 ppm to the ^1H at 3.64 ppm confirms its assignment to T_1H5′/H5″. Likewise, the upfield-shifted C3′ resonance at 72.79 ppm correlates to the upfield H3′ at 4.60 ppm assigned to T_4. Confirmation of the end nucleotide assignments also comes from the 1D carbon spectrum. The 5′-terminal C5′ and the 3′-terminal C3′ signals appear as singlets in the 1D carbon spectrum. The remaining C3′ and C5′ signals are doublets resulting from ^{13}C–^{31}P coupling. The sugar carbon chemical shifts and coupling constants of d(TGGT) are typical of values observed in similar systems.[10]

Assignment of Nonprotonated ^{13}C NMR Signals of d(TGGT). Although it is possible to detect all of the sugar carbon signals from the HMQC experiment, only the G C8, T CMe, and T C6 base carbon signals are observed. Through the use of the ^1H–^{13}C HMBC experiment, it was possible to assign signals for all carbons that are within three bonds of a proton.[10] Thus, only G C2 and G C6 signals could not be assigned.

The true power of the HMBC experiment is the observation of relays between the H1′ and G C4, G C8, T C2, and T C6 signals, which we report here for the first time (Table II). The HMBC spectrum reveals that all of the expected correlations are indeed observed (Figure S1, supplementary material). Since the chemical shifts of the C8 carbons are known from the HMQC experiment, it is possible to assign the G_2 C4 and G_3 C4 signals. In a similar manner, it is possible to assign the T_1 C2 and T_4 C2 resonances. The last assignable G signal type, C5, can be assigned by comparing the observed relays from the H1′ signal with those observed from the H8 signals. From the H8, it is possible to observe correlations to the C4, C5, and C1′. By eliminating the observed relays to the C4 and C1′ signals assigned above, the C5 resonances can be assigned (Table II).

The T C4 and T C5 signals are slightly more difficult to assign. All of the theoretically possible correlations from T H6, which include relays to all of the base carbons and the C1′, are observed in the HMBC spectrum. Of these signals, all were assigned above except for the C4 and C5 signals. Since these signals are not observed under any other experimental conditions, we assign them by analogy to mononucleotide studies,[21] i.e., the C4 resonances

Table II. ^{13}C Chemical Shifts (ppm) of d(TGGT) (1) and d(TGGT)-Pt(en) (2) at 12 °C[a]

	atom type							
	T_1		G_2		G_3		T_4	
	1	2	1	2	1	2	1	2
				Sugars				
C1′	87.45	88.04	85.72	84.58	85.41	84.93	86.95	87.27
C2′	39.31	40.16	38.66	*b*	40.19	40.25	41.61	41.25
C3′	78.90	78.32	79.48	72.83	78.44	78.01	72.51	72.83
C4′	88.67	88.44	87.59	85.36	87.26	87.43	87.05	87.59
C5′	63.97	63.63	68.11	65.05	67.15	67.80	67.74	67.97
				Bases				
C2	154.10	153.71					154.01	153.91
C4	168.59	168.49	154.32	152.75	153.79	153.26	168.62	168.62
C5	114.72	113.76	118.81	116.31	118.62	116.85	114.42	113.94
C6	139.75	139.97					139.70	139.90
C8			139.94	140.18	139.90	140.97		
CMe	14.37	14.50					14.48	14.56

[a] Ethylenediamine signals are observed at 50.50 ppm in the 2D HMQC spectrum. Resonances of G C2 at 156.46 and 156.35 ppm and G C6 at 159.50 and 159.68 ppm were observed in the high-resolution 1D ^{13}C spectrum of d(TGGT) obtained at 22 °C. [b] Not assigned due to peak overlap.

Table III. ^{13}C–^{1}H Coupling Constants of D(TGGT) (1) and d(TGGT)-Pt(en) (2) at 12 °C

	atom type							
	T_1		G_2		G_3		T_4	
	1	2	1	2	1	2	1	2
				Sugars				
C1′	170	165	167	168	167	172	169	171
C2′ (H2′)	138	*a*	132	*a*	135	*a*	133	135
C2′ (H2″)	141	*a*	132	*a*	135	*a*	133	135
C3′	157	155	157	154	155	157	152	154
C4′	152	150	153	148	151	154	147	148
C5′ (H5′)	141	141	146	148	149	*a*	140	*a*
C5′ (H5″)	141	141	148	148	143	*a*	140	*a*
				Bases				
C6	179	181					182	180
C8			215	220	215	220		
CMe	130	130					130	130

[a] Not assigned due to peak overlap.

have chemical shifts that are far downfield from those of C5. It is important to emphasize that not only are correlations from the anomeric protons to the base carbons observed, but correlations from the base protons to the anomeric carbons are also observed.

Assignment of the ^{1}H NMR Signals of d(TGGT)-Pt(en). Assignment of the nonexchangeable protons of the distorted oligonucleotide d(TGGT)-Pt(en) was possible using NOESY, COSY, and HOHAHA techniques in the usual manner. An interesting, extremely broad, temperature-dependent G H1′ resonance[8] is observed upfield at 5.88 ppm; this signal shifted downfield with increased temperature.

The HOHAHA spectrum revealed the *J* networks arising from each of the ribofuranose moieties (Figure S2, supplementary material). Coupled with the NOE data, it was possible to assign all of the nucleotide resonances (Table I). The entire spin families for the three downfield H1′ signals could be assigned from connectivities to the H1′ resonances. No cross peaks were observed, however, to the broad H1′ resonance. COSY connectivities were observed between the broad H1′ signal and the H2′ and H2″ resonances at 2.39 and 2.79 ppm, respectively. These signals in turn had cross peaks to the H3′ signal at 5.24 ppm. The H3′ showed connectivity to the rest of the members of the *J* network in the HOHAHA spectrum.

Assignment of the Protonated ^{13}C NMR Signals of d(TGGT)-Pt(en). All the protonated carbon resonances except for G_2 C2′, which was overlapped with other C2′ signals, were assigned with the ^{1}H–^{13}C HMQC data as outlined above (Table II).

Assignment of the Nonprotonated ^{13}C NMR Signals of d(TGGT)-Pt(en). The nonprotonated base carbon signals were all observed in the HMBC spectrum, allowing assignments to be made as described above. The connectivities with the H1′ and C1′ signals were observed for the T nucleotides. However, these cross peaks were absent for the G nucleotides. This absence of cross peaks is most probably a result of unfavorable coupling constants resulting from the unique dihedral angles caused by platination. These cross peaks were not needed for the assignments because the G C4 and G C5 signals are easily identified on the basis of chemical shift.

Discussion

The goals of this study can be enumerated as follows: (1) to evaluate the prediction of the Harbison model on the dependence of deoxyribose ^{13}C shifts on sugar pucker, (2) to assess the effects of an inertly attached metal center on ^{13}C shifts of bases, and (3) to determine whether ^{1}H–^{13}C coupling between nucleic acid base carbons H1′ and between C1′ and base aromatic protons could be used in signal assignment. The largest measure of success was achieved in the first objective.

The change in the C3′ chemical shift at 12 °C of G_2 by 6.6 ppm to higher field (Table II) is a clear indication of the predictive power of the Harbison method. The results suggest strongly that the G_2 sugar is in an N-type conformation most of the time, since a shift of ~7.7 ppm is predicted for a C2′ endo → C3′ endo conformational change. The ~2.2 and 3.1 ppm upfield shifts of C4′ and C5′, respectively, compared favorably but less well with the expected 0.9 and 4.3 ppm shifts expected from a C2′ endo → C3 endo′ conversion. The shift of the C4′ signal is too far upfield for any A- or B-DNA conformation for which shift values were predicted by Harbison. This result at 12 °C strongly suggests that the G_2 sugar is not interconverting between C2′ endo and C3′ endo conformations but has adopted a different N-type conformation or is equilibrating between two conformers, one of which is neither C2′ or C3′ endo.

To examine this question further, we also examined the ^{13}C spectrum of d(TGGT)-Pt(en) at 40 °C. At this temperature, the usually broad G_2 H1′ signal[5-8] becomes sharper, exhibits a normal doublet of doublets coupling pattern, and is observed in a normal shift region (Figure 1). Despite these dramatic changes in signal shape and shift in the ^{1}H spectrum, the ^{13}C spectrum changes very little between 12 and 40 °C (Figure 2). This insensitivity of the ^{13}C spectrum to temperature change can be contrasted with the dramatically different shifts for the G_2 sugar compared to the G_3 signals, to internal sugars in other oligonucleotides, and to the G_2 and G_3 sugars in unplatinated d(TGGT) (Figure 3). These comparisons suggest that, although there is a large conformational change induced by platination, this change is not temperature dependent over the range studied here. The changes in the ^{1}H NMR spectrum probably result from other changes in conformation, possibly from changes in the glycosyl torsion angle χ or from changes in the dihedral angle between the guanine bases or those between the bases and the coordination plane.

(21) Breitmaier, E.; Voelter, W. *^{13}C NMR Spectroscopy*; Verlag Chemie: New York, 1978; p 270, and references therein.

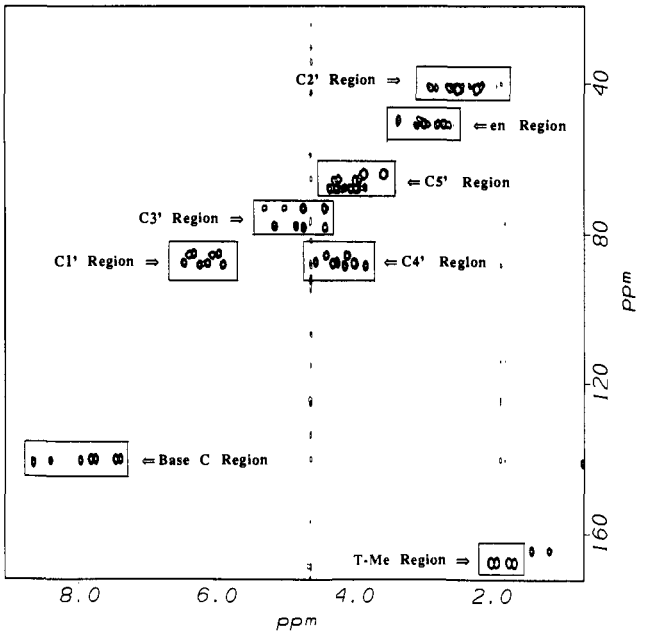

Figure 1. Full HMQC spectrum of d(TGGT)-Pt(en) obtained at 40 °C. Boxes highlight specific spectral regions, and demonstrate that spectral overlap in the ^1H dimension can be resolved in the ^{13}C dimension (e.g., H4′, H5′/H5″ are overlapped, whereas C4′ and C5′ are clearly resolved.)

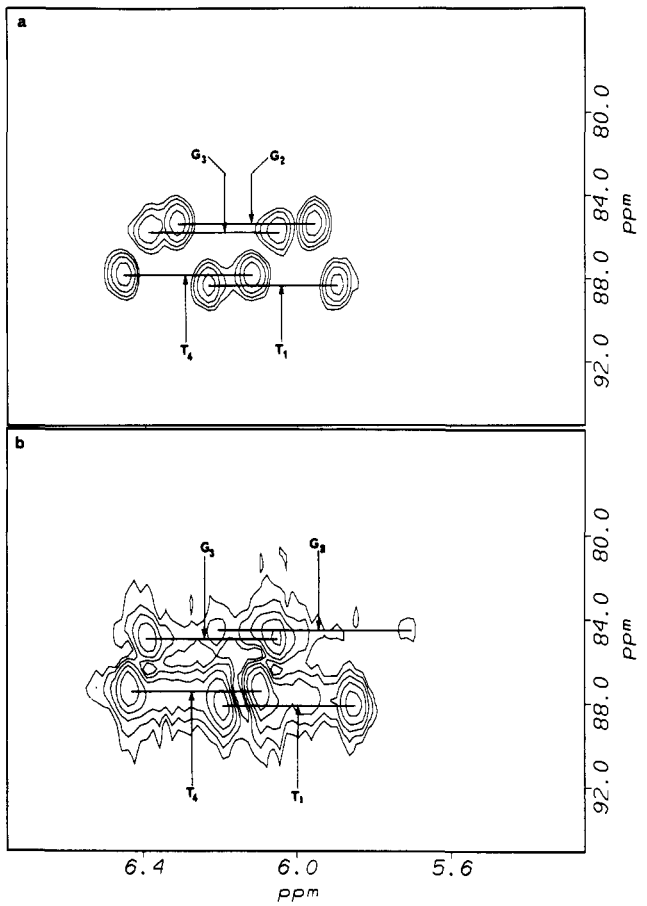

Figure 2. Enlargements of the H1′–C1′ regions of the HMQC spectra of d(TGGT)-Pt(en) at (a) 40 °C and (b) 12 °C. Note the lack of temperature dependence of the G_2 H1′ resonance.

These conclusions can be tested by evaluating the C3′ shift of the 5′G sugar of d(GG)-*cis*-Pt$(NH_3)_2$. The conformation of the 5′G sugar in the latter species over a range of temperatures (23, 53, and 81 °C) has been carefully studied by ^1H NMR spectroscopy.[22] This is possible because the 5′G H1′ signal is not very broad as in the case of longer single-stranded oligonucleotides. Analysis of the ^1H–^1H coupling constants led to the conclusion that the species is exclusively N with a pseudorotation angle $P = 1° (\pm 7°)$. This value could represent a conformational average between two N-type conformers. We assigned the ^{13}C signal of C3′ of the 5′G by HMQC methods, using the reported ^1H assignments. The values obtained at 23 and 53 °C were 73.03 and 73.21 ppm. The average value of these shifts, 73.12 ppm, agrees most favorably with the average value of 73.04 ppm obtained for the G_2 C3′ signal of d(TGGT)-Pt(en).

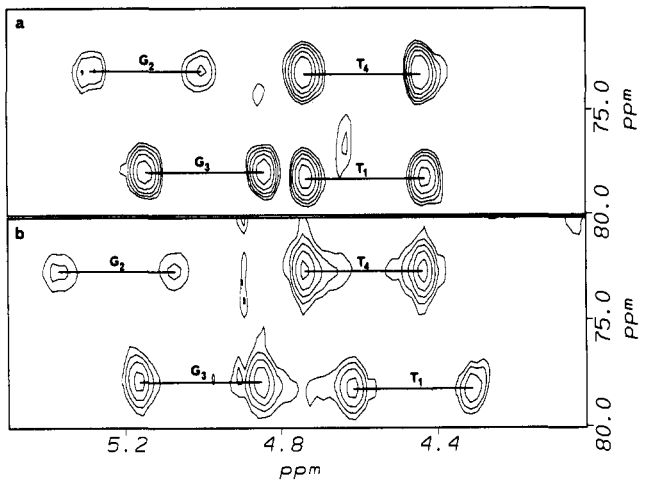

Figure 3. Enlargements of the H3′–C3′ regions of the HMQC spectra of d(TGGT)-Pt(en) at (a) 40 °C and (b) 12 °C showing upfield ^{13}C chemical shift of G_2 C3′ vs other C3′ signals. The T_4 C3′ signal is upfield as expected because it is the 3′-terminal residue.

Further evidence in support of the above interpretation can be found in the X-ray structural results for d(pGG)-*cis*-Pt$(NH_3)_2$.[23] This adduct crystallizes with four different species in the unit cell. However, half of these species have a $P \cong -15.5°$ and the other half have a $P \cong 21.5°$, i.e., an average $P = 3°$ in agreement with the ^1H NMR study of d(GG)-*cis*-Pt$(NH_3)_2$.[22] Together, these results suggest that, in d(TGGT)-Pt(en), the average conformation of the 5′G has $P \cong 0$ and that this average is not temperature dependent.

A second objective of the study was to assess the utility of ^{13}C NMR to identify metal binding sites in distorted oligonucleotides. It has been established that ^{13}C NMR is a more useful method than ^1H NMR in assessing binding sites of labile metal species[24,25] since ^{13}C signals shift in characteristic patterns of upfield and downfield shifts and since the number of ^1H signals for any given nucleobase is limited. Proton NMR spectra are useful for inert Pt(II) species since pH titrations can be performed without disrupting the metal–ligand bond.[6,7] For guanine derivatives, however, only one base ^1H signal is observable in D_2O. Moreover, oligonucleotide G H8 signals shift in a manner not completely understood.[7]

A recent study has reported the effect of the *cis*-Pt$(NH_3)_2$ moiety in the ^{13}C signals of guanosine in DMSO-d_6.[14] The pattern of shifts was characteristic of metal binding of N7 with C8 downfield shifts of 3.6 ppm and C5 and C4 upfield shifts of 3.0 and 1.3 ppm, respectively. We found that the C5 and C4 signals of the platinated G's shifted upfield by an average of 2.1 and 1.1 ppm, respectively. However, the C8 signals, in our case, shifted

(22) den Hartog, J. H. J.; Altona, C.; Chottard, J.-C.; Girault, J.-P.; Lallemand, J.-Y.; de Leeuw, F. A. A. M.; Marcelis, A. T. M.; Reedijk, J. *Nucleic Acids Res.* **1982**, *10*, 4715.
(23) Sherman, S. E.; Gibson, D.; Wang, A. H.-J.; Lippard, S. J. *J. Am. Chem. Soc.* **1988**, *110*, 7368.
(24) Marzilli, L. G.; Stewart, R. C.; Van Vuuren, C. P.; de Castro, B.; Caradonna, J. P. *J. Am. Chem. Soc.* **1978**, *100*, 3967. Marzilli, L. G.; de Castro, B.; Caradonna, J. P.; Stewart, R. C.; van Vuuren, C. P. *J. Am. Chem. Soc.* **1980**, *102*, 916. Marzilli, L. G.; de Castro, B.; Solorzano, C. *J. Am. Chem. Soc.* **1982**, *104*, 461. Marzilli, L. G. *Progress in Inorganic Chemistry*; Lippard, S. J., Ed.; Wiley-Interscience: New York, 1977; Vol. 23, p 255.
(25) Jia, X., Zon, G., Marzilli, L. G. *Inorg. Chem.* **1991**, *30*, 228.

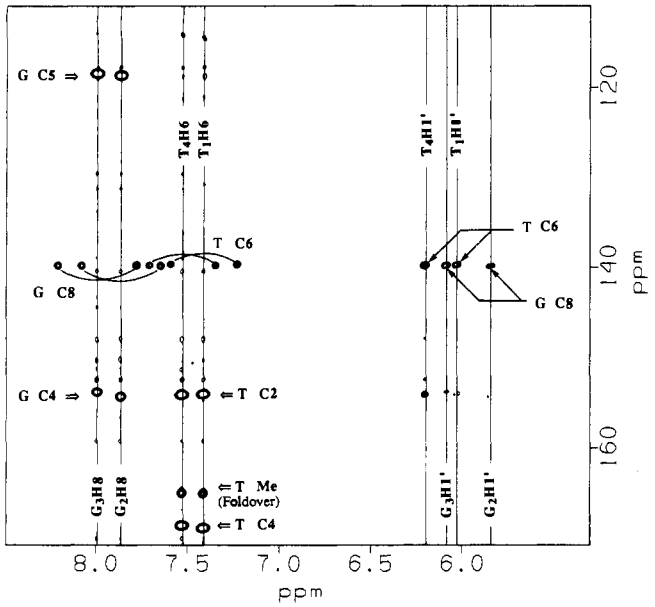

Figure 4. Expansion of the HMBC spectrum of d(TGGT) at 12 °C highlighting observed correlations between base carbons and the signals of the H1′ and the nonexchangeable base protons. Correlations are observed between G H8–G C8 and T H6–T C6 due to incomplete cancellation of single-bond coupling.

downfield relatively little. Probably for the same reason that the shifts in the H8 signals are not fully understood,[7] the C8 shifts of the oligonucleotide do not appear to follow expected trends based on mononucleoside data. It should be pointed out that the cross-linked structure is quite distorted[23,26,27] and the ideal overlap of the N7 lone pairs of both guanines with the metal center cannot be achieved. Furthermore, heavy-atom anisotropic effects of the Pt can influence the ^{13}C shift.[28] In retrospect, it is not surprising that the C8 shifts are not useful in this case. The C5 signals *does* shift in the characteristics way, presumably because of the distance of this C from the Pt center. This similarity suggests that the Pt(II) can still influence the electronic distribution in the base in a manner similar to that in mononucleotides. The change in the C8–H8 coupling appears to be too small to be useful in identifying metal binding sites.

A third objective of this study was to determine if H1′ coupling to base carbons and base H8 or H6 coupling to C1′ could be useful in unambiguously correlating a given base with a given sugar. We feel that such an unambiguous correlation would be useful in confirming signal assignments for highly distorted and highly flexible structures. This base proton to C1′ coupling was observed for all four nucleotides in d(TGGT) (Figure 4). The ability to observe these correlations that are based on scalar coupling, and not upon through-space interactions, eliminates the need for assumptions about structural conformation that are implicit to assignments based on 2D NOE data. In d(TGGT)-Pt(en), however, we were able to observe correlations for the two T nucleotides. Thus, the method has potential for loop regions of hairpins, but may not be applicable to nucleotides greatly distorted by anticancer drug adduct formation. The method does confirm the assignment of some of the nucleotides, thereby limiting the uncertainty in the assignments of the remaining nucleotides. The absence of observed coupling in d(TGGT)-Pt(en) lends support to the evidence that there is a structural distortion at the platination site.

An initial qualitative structure of the d(TGGT)-Pt(en) system, model I, is illustrated in Figure 5 and in Figure S4 (supplementary material). The model is based on the coordinates of the d-

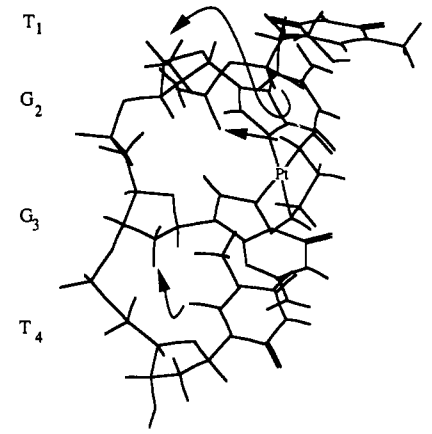

Figure 5. Idealized initial structural model d(TGGT)-Pt(en). The curved arrows indicate the locations of interresidue NOEs observed between terminal nucleotides and internal nucleotides. The straight arrow highlights possible hydrogen-bonding interaction between an amine proton and a phosphate oxygen.

(pGG)-*cis*-Pt$(NH_3)_2$ crystal structure.[23] The program MacroModel[29] was used to modify the X-ray structure. Thymine nucleotide units were added to the 3′- and 5′-terminal ends of the adduct, and the relevant sugar phosphate torsion angles ($\alpha \rightarrow \zeta$)[30] were adjusted. Torsion angles $G_2\,\beta \rightarrow G_3\delta$ were set at the crystal structure values, while the torsion angles from $T_1\beta \rightarrow G_2\alpha$ and $G_3\epsilon \rightarrow T_4\delta$ were assigned the B-form values reported by Lippard.[23] In addition to these modifications, the NH_3 ligands of the Pt center were replaced by the bidentate en ligand. The resulting reduction in N–Pt–N bond angle between the amine nitrogens (90° → ~86°), and the corresponding increase in the N7–Pt–N bond angles (90° → ~91.5°), were included in the model. The expected C3′ endo deoxyribose conformation of G_2, the head-to-head arrangement of the guanines, and the hydrogen bond between the amine nitrogen and an oxygen of the G_2 5′-phosphate are incorporated into the model.

Only two, highly unusual NOE connectivities were observed between the terminal T residues and the central nucleotides. One of these NOE enhancements occurred between the T_1 H3′ and G_2 H5′/H5″ signals. The initial model I does not explain this observation. Of the six sugar phosphate torsion angles between the T_1 and G_2 residues, only α and ζ, which define rotation about P–O bonds, are typically observed to demonstrate rotational variability; the remaining angles show very high specificity toward given rotational forms.[31] With an Evans & Sutherland PS390 graphics terminal, we performed real-time rotations of both the α and ζ torsion angles simultaneously through an entire 360° rotation; the other torsion angles were restricted to their preferred values. With this approach, it was not possible both to maintain an optimal amine–phosphate H-bond interaction and to position the T_1 and G_2 residues in a conformation consistent with the observed NOE enhancement. However, if the H bond is not maintained, several conformations would exhibit the weak T_1 H3′ to G_2 H5′/H5″ NOE. If the H bond is maintained, it is possible to explain the NOE result only by utilizing torsional angles that are outside the normally observed range.

The other interresidue NOE enhancement was observed between T_4 H6 and G_3 H1′. In addition, the expected NOE correlations between the T_4 H6 and T_4 Me to G_3 H2′/H2″ were lacking. Rotation of the α and ζ torsion angles as well as χ[30]

(26) Sherman, S. E.; Gibson, D.; Wang, A. H.-J.; Lippard, S. J. *Science* **1985**, *230*, 412.
(27) Admiraal, G.; van der Veer, J. L.; de Graaff, R. A.; den Hartog, J. H. J.; Reedijk, J. *J. Am. Chem. Soc.* **1987**, *109*, 592.
(28) Sundquist, W. I.; Lippard, S. J. *Coord. Chem. Rev.* **1990**, *100*, 293.
(29) Still, W. C.; Mohamdi, F.; Richards, N. G. J.; Guida, W. C.; Lipton, M.; Liskamp, R.; Chang, G.; Hendrickson, T.; DeGunst, F.; Hasel, W. *MacroModel V 2.5*; Department of Chemistry, Columbia University: New York, 1988.
(30) The sugar phosphate torsion angles are described as follows: P–α-O5′–β-C5′–γ-C4′–δ-C3′–ϵ-O3′–ζ-P. The glycosyl torsion angle, χ, is defined as O4′–C1′–χ–N9–C4 for G, and O4′–C1′–χ–N1–C2 for T. The eclipsed position represents a 0° value and positive values refer to clockwise rotation of the rear bond relative to the front bond.[31]
(31) Saenger, W. *Principles of Nucleic Acid Structure*; Springer-Verlag: New York, 1984; pp 9–104.

through 360° did not reveal a single conformation that explains all of the observed data. Thus, both ends of the oligonucleotide are flexible and exist in a mixture of conformers.

Three additional qualitative models, models II–IV, were also constructed and examined. The values of the torsion angles used to construct the various structures are listed in Table SIV (supplementary material). For example, model III made use of the A- and B-DNA torsion angles reported by Lippard (Figure S5, supplementary material).[23] No noteworthy differences were observed for models II–IV compared to model I. Thus, our conclusions based on our initial qualitative model I appear reasonable.

In summary, the use of ^{13}C NMR spectroscopy to study drug–oligonucleotide adducts holds considerable promise. The method clearly pinpoints sugar conformational changes. A predominantly S → predominantly N conformational change shifts the ^{13}C signal of C3′ into a spectral region of the 2D HMQC spectrum that otherwise lacks signals except for the 3′-terminal C3′ signal. Thus, it is possible that such a conformational change can be observed in relatively large oligonucleotides where ^1H signal overlap would prevent assessment of ^1H–^1H coupling constants, which otherwise are useful for assigning sugar pucker. Furthermore, as in the case of cross-linked adducts studied here, the ^1H–^1H coupling pattern may not be resolved, precluding the use of this method for assigning sugar pucker. Clearly, the ^1H and ^{13}C methods are complementary and both can be very useful. Finally, ^{13}C signals are useful in defining metal-binding sites. The same advantages of this method for mononucleotide studies are passed on to oligonucleotide studies.[25] Signals for carbons remote from the metal binding site appear to be most useful.

Acknowledgment. We thank the National Institutes of Health for support (GM 29222 to L.G.M.), as well as for partial support for the instrument purchase, which was also supported in part by the National Science Foundation. We acknowledge several helpful discussions with Prof. David Live.

Registry No. d(TGGT), 87471-59-8; $Pt(en)Cl_2$, 14096-51-6; d(TGGT)-Pt(en), 132260-29-8.

Supplementary Material Available: Tables of the ^1H and ^{13}C chemical shifts and the ^{13}C–^1H coupling constants of d(TGGT)-Pt(en) at 40 °C and of the torsional angles used for models I–IV and figures of the full HMBC spectrum of d(TGGT) at 12 °C, the sugar region of the HOHAHA spectrum of d(TGGT) at 40 °C, the full NOESY spectrum of d(TGGT)-Pt(en) at 12 °C, and structural models I and III (10 pages). Ordering information is available on any current masthead page.

η^2-Dihydrogen on the Brink of Homolytic Cleavage: *trans*-$[Os(H\cdots H)H(PEt_2CH_2CH_2PEt_2)_2]^+$ Has Spectroscopic and Chemical Properties between Those of the Isoelectronic Complexes *trans*-$[OsH(PPh_2CH_2CH_2PPh_2)_2(\eta^2\text{-}H_2)]^+$ and $ReH_3(PPh_2CH_2CH_2PPh_2)_2$

Kelly A. Earl, Guochen Jia, Patricia A. Maltby, and Robert H. Morris*

Contribution from the Department of Chemistry and the Scarborough Campus, University of Toronto, Toronto, Ontario M5S 1A1, Canada. *Received September 5, 1990*

Abstract: The new, octahedral complex *trans*-$[OsH(dppe)_2(\eta^2\text{-}H_2)]^+$, **1Os**, dppe = $PPh_2CH_2CH_2PPh_2$, prepared by addition of H^+ to *cis*-$OsH_2(dppe)_2$, has a rapidly spinning dihydrogen ligand with an unusually long (0.99 Å) H–H distance according to the T_1 NMR method. Additional evidence for this is a short T_1 value for the H_2 ligand in the complex *trans*-$[OsH(dppe\text{-}d_{20})_2(\eta^2\text{-}H_2)]^+$ and a large $^1J(H,D)$ value (25.5 Hz) for *trans*-$[OsH(dppe)_2(\eta^2\text{-}HD)]^+$, **1Os**-$d_1$. The known complex *trans*-$[Os(H\cdots H)H(depe)_2]^+$, **2Os**, depe = $PEt_2CH_2CH_2PEt_2$, has properties (δH, $J(H,D)$, T_1^{-1}) between those of **1Os** and $ReH_3(dppe)_2$, **3Re**, a true pentagonal, bipyramidal trihydride with $r(H\cdots H) \sim 2$ Å; e.g., the $J(H\cdots D)$ coupling for *trans*-$[Os(H\cdots D)D(depe)_2]^+$, **2Os**-$d_2$, is the unusual value of ~11.5 Hz, whereas for **3Re**-d_2 it is 0 Hz, as expected. Significantly the 11.5-Hz value varies by ±1 Hz depending on the solvent and temperature. VT NMR spectra of **2Os**-d_2 conclusively show that $J(H\cdots D)$ is not lost but is averaged by intramolecular H/D atom exchange; at 325 K, $J_{av}(H,D) = 3.8$ Hz. There are three possible answers to the question as to whether there is homolytic cleavage of H_2 in **2Os**: (1) no H–H cleavage so that **2Os**, like **1Os**, has a stretched, rapidly spinning dihydrogen ligand with $r(H\text{–}H) = 1.2$ Å; (2) complete H–H bond breaking to give an unusual trihydride with two closely spaced hydrides, 1.4–1.5 Å apart; and (3) a rapidly equilibrating mixture ($\Delta G^{\ddagger} \leq 9$ kcal mol^{-1}) of $Os(H)(\eta^2\text{-}H_2)$ and $Os(H)_3$ tautomers. The rapid equilibrium model (3) with the $Os(H)_3$ tautomer in greater abundance fits all available data for **2Os** and other complexes of Os with small $J(H\cdots D)$ couplings. The equilibrium shifts toward the dihydrogen form with an increase in temperature or on going from acetone-d_6 to CD_2Cl_2 as signaled by changes in $\delta(H_2)$, $T_1(H_2)$, and $J(H,D)$ values. An alternative answer (2) cannot be ruled out since closely spaced hydrides might move closer together with these changes in conditions and produce the same spectral changes. Also included are X-ray diffraction structural data for the three complexes, their infrared, chemical, and electrochemical properties as well as differences in NMR properties: rates of intramolecular H-atom exchange, chemical shifts, and coupling constants of the isotopomers **1Os**-d_1, **2Os**-d_1, **2Os**-d_2, and **3Re**-d_2. **1Os** retains the H–H bond because it has lower energy 5d electrons than **2Os** or **3Re**, and the dppe ligands are small enough to allow an undistorted octahedral coordination geometry. **3Re** gives shorter T_1 times for hydride and phosphorus nuclei than expected solely from dipolar relaxation by neighboring protons.

Several η^2-dihydrogen complexes have characteristics indicative of a short (<1 Å) H–H distance and a relatively weak interaction with the metal.[1-8] The large dipolar coupling between the η^2-H_2 nuclei can be observed by NMR in the solid state,[9] and this

0002-7863/91/1513-3027$02.50/0